

On coherent structures in the compressible turbulent round jet

By P. REYNIER AND H. HA MINH

Institut de Mécanique des Fluides de Toulouse,
Avenue du Pr. Camille Soula, 31400 Toulouse, France

(1997)

The presence of two-dimensional coherent structures in the near-field of the round jet has been established by several experimental investigations and direct Navier-Stokes simulations (DNS). Their study has a great importance to improve the prediction of unsteady flows dominated by large scale structures. Indeed, coherent structures play a determinant role on turbulence and flow evolution. The goal of this numerical study is to apply the semi-deterministic modelling, a method close to the large eddy simulation (LES), to the simulation of compressible round jets. This allows the simulation of natural unsteadiness without any flow excitation. A free jet configuration is computed for three Mach numbers of 0.3, 0.96 and 1.5 to evaluate the influence of compressibility effects on instability, Strouhal number and expansion rate. There is not quantitative comparisons on flow quantities with experimental data, except for the Strouhal number, due to the discrepancies between the configuration computed here and those experimentally investigated in past studies. The numerical results on coherent structures are validated across a comparison on the Strouhal number of the preferred mode. The results on the evolution of the Strouhal number with the Mach number are in excellent agreement with previous experiments. Moreover, the evolution of the large scale vortices in the flow is well correlated by experimental and DNS results obtained on other configurations.

1. Introduction

Since the pioneering works of Rayleigh (1879) the jet instability has been the matter of many experimental and theoretical studies (e.g. Crow & Champagne 1971; Lau & Fisher 1975; Hussain & Zaman 1981; Sokolov, Kleis & Hussain 1981; Liepmann & Gharib 1992). All these studies turned on the investigation on large scale structures in the round jets. The coherent structures such as they have been defined by Hussain (1983, 1986) exist in the round jet as in any flow including a mixing layer. Their discovery in the near-field of the axisymmetric jet is the fact of Crow & Champagne (1971). Their works put in evidence a preferred mode for this flow with an associated Strouhal number of about 0.3. Later, Hussain & Zaman (1981) investigated more largely this preferred mode and established its independence with the initial boundary layer instability. Indeed, the characteristic length of this mode is not the boundary layer thickness at the inlet pipe but the jet diameter. Large scale vortices evolve in the jet shear-layer and Lau & Fisher (1975) showed that the basic structure of the turbulent round jet consists essentially in an alley of vortices moving downstream in the mixing layer.

In the round jet, the entrainment process is drastically influenced and increased by the large scale structures evolving in the shear-layer (see Liepmann & Gharib 1992). In this way, if the entrainment is constant in the far-field, it increases in the near-field. Ricou &

Spalding (1961) suggested a linear growth for $x/D \leq 5$ which agrees with the experimental results of Liepmann & Gharib (1992). For Bogulawski & Popiel (1979), the entrainment rate is constant in the near region. This discrepancy between these experimental results can be explained by different inlet conditions: in the experiment of Bogulawski & Popiel (1979) the flow is fully-developed whereas in that of Liepmann & Gharib (1992) the turbulence level at the exit is lower (young turbulence). Moreover, these last authors established that the entrainment capacity of a laminar or transitional jet is larger than that of a fully-developed turbulent jet. This is a consequence of the presence of coherent structures which carry some fluid across the jet interface involving a large growth of the shear-layer. On the other hand, these vortices increase the interface length, therefore the diffusion between the jet and the outer environment.

If the greater part of experiments on jet instabilities have been carried out for low or moderate Reynolds numbers and incompressible flows (Crow & Champagne 1971; Lau & Fisher 1975; Hussain & Zaman 1981), some studies have been led for high Reynolds number or compressible flows (e.g. Arnette, Samimy & Elliot 1993; Fourgnette, Mungal & Dibble 1991; Lepicovski *et al.* 1987). They established the existence of coherent structures even for high Mach numbers: 2.5 in the experiment of Morrison & McLaughlin (1980). Moore (1977) had already demonstrated that the large scale structures present at low Reynolds numbers (10^4) are also observed at Reynolds numbers of about 10^6 . These coherent structures, present in the mixing layer of the jet, play a central role in the flow, revealed by the fundamental works of Brown & Roshko (1974) and Winant & Browand (1974) on the compressible mixing layer. The two-dimensional coherent structures and their relation to the hydrodynamic instability have been studied for the following reasons:

- Their role in the laminar-turbulent transition;
- The interest for the theoretical modelling to improve the prediction of flow and mixing.

The vortices evolving in the shear-layer originate from instability waves of which the growth is ensured by the nonlinear interactions of the flow. This phenomenon has been experimentally investigated by Liepmann & Gharib (1992) and numerically by Verzicco & Orlandi (1994) and Grinstein, Oran & Hussain (1987) for incompressible and compressible jets. There are few studies on instability waves in compressible jets. Indeed, the measurements on pressure and velocity fluctuations, more particularly in supersonic flows, do not give impressive results which explains the restricted number of experiments carried out. However, Oertel (1982) and Tam & Hu (1989) observed that three different families of instability waves, with distinct wave patterns and propagation characteristics, are present in supersonic jets:

- The Kelvin-Helmholtz instability;
- The subsonic waves (waves with subsonic phase velocities);
- The supersonic waves (waves with supersonic phase velocities).

These three modes of instability modes are convective. Tam & Hu (1989) did not observe absolute instabilities in their investigations. When the jet is subsonic, only the Kelvin-Helmholtz instability is active. This phenomenon is independent from the Reynolds number: Lepicovski *et al.* (1987) showed that Kelvin-Helmholtz instability waves are present at Reynolds numbers higher than 10^6 . On the other hand, the growth rate of this instability kind decreases when the Mach number increases (Miles 1958). The subsonic waves are present for low supersonic jets, the last mode of instability, the supersonic waves, is present if only the Mach number is higher than the sum of ambient and jet speeds of sound (Tam & Hu 1989).

In the present paper only the Kelvin-Helmoltz instability is simulated. The involving waves are at the origin of the coherent structures which control the dynamic and the mixing of the jet. According to Tam & Hu (1989) the flow is dominated by a similar process for low and moderate supersonic Mach numbers. Zhou & Lin (1992) showed that the large scale vortices originate from pressure fluctuations at the jet interface. The results of Michalke (1984), Liepmann & Gharib (1992) and Verzicco & Orlandi (1994) show that the shear-layer becomes unstable near the inlet then rolls up to form vortex rings and finally turns fully turbulent.

The mixing layer vortices appear before $x/D=2$ (e.g. Arnette *et al.* 1993; Grinstein *et al.* 1987; Liepmann & Gharib 1992), next both contraction and expansion enhance the evolution of three-dimensional secondary structures. The experimental investigation of Liepmann & Gharib (1992) as well as the DNS results of Verzicco & Orlandi (1994) show that three-dimensional structures in finger-form appear on the edges of the two-dimensional vortices with fluid ejection in the shape of lateral jets. These three-dimensional effects are strong downstream the potential core at $4D \leq x \leq 5D$ (e.g. Moore 1977; Sokolov *et al.* 1981; Grinstein *et al.* 1987; Liepmann & Gharib 1992). They result from the strongly nonlinear interactions of the flow-field. In supersonic jets, the three-dimensional unsteadiness have been observed at the end of the potential core by Morrison & McLaughlin (1980). For Fourguette *et al.* (1991) the supersonic jets are more three-dimensional than incompressible jets, due to oblique instability waves in the flow. Clemens & Mungal (1992) and Samimy, Reeder & Elliot (1992) have also noted the same phenomenon in the compressible mixing layer. The stability analysis of Ragab & Wu (1989) shows that the oblique instability modes are more amplified than the two-dimensional modes in highly compressible flows.

The aim of this paper is essentially to improve the prediction of the jet near-field, especially taking into account the two-dimensional coherent structures. The three-dimensional aspects will not be tackled here. For the turbulence modelling, since DNS and LES are not available for the numerical computation of high Reynolds jets, the semi-deterministic approach developed by Ha Minh & Kourta (1993) and already applied to the simulation of coaxial jets by Reynier & Ha Minh (1995) has been chosen. This method is close to the LES but differs slightly by its spirit. The main purpose of this work is to apply the semi-deterministic modelling (SDM) to simulate natural flow unsteadiness in a compressible round jet. Therefore, main features on coherent structures as their evolution in the flow and their interaction with the mean quantities are studied. Moreover, the influence of compressibility effects on coherent structures and Strouhal number is evaluated. So, several calculations have been led on the same configuration for several Mach numbers, they allowed the prediction of dynamic and energetic quantities in the computational flow. Finally, to verify the trends observed, these numerical results are qualitatively compared to those of experimental and DNS investigations.

2. Methodology

2.1. The semi-deterministic modelling

Most of flows contain organized and random (in the sense of chaotic) characters. For a long time, the numerical predictions have been limited to the calculation of approached problems (Prandtl approximation) where the flow unsteadiness is not considered. So, the spreading out of the turbulence closures in the seventies has been built on the resolution under these approximations. Therefore, turbulence statistical models lead to satisfying results when the turbulent energy is in spectral equilibrium, the turbulence is then fully-

developed. However, many flows particularly in industrial problems are rather concerned by young turbulence (i.e. near the transition). This last is characterized by two main features:

- The turbulence may be at low turbulent Reynolds numbers so the turbulent and molecular diffusions may be of the same order;
- The three-dimensional spectrum of the energy is not in equilibrium, it is strongly modified by the presence of unsteady organized structures.

These organized structures constitute the coherent part of the turbulence. They are highly dependent on initial and boundary conditions and they strongly influence the turbulence energetic level. Indeed, Hussain & Zaman (1981) and Sokolov *et al.* (1981) remarked in their experimental investigations on round jets (with inlet conditions characterized by low turbulence levels) that near the exit the coherent part of the turbulent energy is greater than the random component. Therefore, the classical statistical modelling need to be reconsidered to take account of the organized unsteadiness.

Reynolds & Hussain (1972) demonstrated that every instantaneous physical quantity $f(x_k, t)$ can be split in three components:

$$f(x_k, t) = \underbrace{\bar{f}(x_k)}_{(a)} + \underbrace{f_c(x_k, t)}_{(b)} + \underbrace{f_r(x_k, t)}_{(c)} \quad (2.1)$$

The part (a) represents the time-averaged quantity. It is generally the only quantity available from experiment. The coherent or organized unsteadiness (b) possesses a determinist character available from numerical calculations. Coherent unsteadiness is highly dependent on the fundamental properties of the flow: geometry, boundary and initial conditions and physical properties of the fluid medium. The component (c) points out the random or incoherent fluctuations. The corresponding structures are characterized by a continuous spectrum which some peaks, traces of organized structures may be surimposed. In theory, the simulation of all vortices (DNS) even for small scales is possible. But, if DNS is the most natural way to predict a flow, the computation cost of this pure approach is too expensive for high Reynolds number flows. Finally, the parts whose the computation can be reasonably expected are the time-averaged motion and the coherent unsteadiness. A new quantity, the phase average, is obtained. Determined from the successive coherent structures at the same age (or phase) of their evolution, its expression is:

$$\langle f(x_k, t) \rangle = \bar{f}(x_k) + f_c(x_k, t) \quad (2.2)$$

so,

$$f(x_k, t) = \langle f(x_k, t) \rangle + f_r(x_k, t) \quad (2.3)$$

If $f_r = 0$, the DNS is found. The case where f_r is very small corresponds to the LES approach. Finally, if the quantity $\langle f(x_k, t) \rangle$ is minimized and reduced to the time average, the classical statistical approach is obtained. Also, the SDM appears as an intermediate way between the classical statistical modelling and the DNS. Although this approach is very close to the LES, several differences exist between these two methods. From the methodology point of view some questions on the necessity to distinguish LES and SDM can be legitimately set. In the formalism field, the equations to solve for the two methods are the same. Indeed, the phase average leads to the same equations that the classical modelling. The only differences in the governing equations come from the closure, sub-grid modelling for the LES while f_r is represented by a turbulence model in SDM. The main discrepancy between the two approaches is the splitting used for the vortical

structures. The LES splits the structures according to their size: large scale structures to be simulated and small scale structures to be modelled. SDM splits the vortices in function of their nature: coherent structures to be computed and random turbulence to be modelled. If the coherent structures have a highly two-dimensional character, a two-dimensional approach much economical can be used with SDM, while LES must use three-dimensional calculations. As the part to model contains all the random components the situation is nearly identical to the classical modelling. The governing equations are similar, so the use of the same process to built the new closures is tempting. However, some modifications must be done in the set of constants. According to Ha Minh & Kourta (1993), as the turbulence role has been defined again, the constants must be recalibrated.

2.2. Governing equations

The near-field of the round jet is highly influenced by the presence of two-dimensional large coherent structures if the initial conditions allow it (under-developed turbulence or laminar flow), so the present study is limited to the two-dimensional aspect of this flow. The governing equations are the unsteady Navier-Stokes equations written in axisymmetric coordinates with the mass-weighted average of Favre (1965) and a state equation for a perfect gas. The closure is obtained using a $k - \epsilon$ turbulence model. The governing equations for the conservation of density $\bar{\rho}$, pressure \bar{P} , momentum $\bar{\rho}\tilde{U}$ in streamwise direction x , momentum $\bar{\rho}\tilde{V}$ in spanwise direction r and total energy \tilde{E} (the equations of the turbulence model will be presented in § 2.3) are

Equation for the conservation of the mass-density $\bar{\rho}$

$$\frac{\partial}{\partial t}\bar{\rho} + \frac{\partial}{\partial x}\bar{\rho}\tilde{U} + \frac{1}{r}\frac{\partial}{\partial r}r\bar{\rho}\tilde{V} = 0 \quad (2.4)$$

Equation for the conservation of the momentum $\bar{\rho}\tilde{U}$

$$\begin{aligned} \frac{\partial}{\partial t}\bar{\rho}\tilde{U} + \frac{\partial}{\partial x}\left\{\bar{\rho}\tilde{U}\tilde{U} + \frac{2}{3}\bar{\rho}\tilde{k} + \bar{P} - (\mu + \mu_t)\tilde{S}_{xx}\right\} \\ + \frac{1}{r}\frac{\partial}{\partial r}r\left\{\bar{\rho}\tilde{U}\tilde{V} - (\mu + \mu_t)\tilde{S}_{rx}\right\} = 0 \end{aligned} \quad (2.5)$$

Equation for the conservation of the momentum $\bar{\rho}\tilde{V}$

$$\begin{aligned} \frac{\partial}{\partial t}\bar{\rho}\tilde{V} + \frac{\partial}{\partial x}\left\{\bar{\rho}\tilde{U}\tilde{V} - (\mu + \mu_t)\tilde{S}_{xr}\right\} \\ + \frac{1}{r}\frac{\partial}{\partial r}r\left\{\bar{\rho}\tilde{V}\tilde{V} + \bar{P} + \frac{2}{3}\bar{\rho}\tilde{k} - (\mu + \mu_t)\tilde{S}_{rr}\right\} = \\ \frac{1}{r}\left\{\tilde{P} + \frac{2}{3}\bar{\rho}\tilde{k} - (\mu + \mu_t)\tilde{S}_{\theta\theta}\right\} \end{aligned} \quad (2.6)$$

The terms of the strain tensor are given by the following expressions:

$$\tilde{S}_{rr} = 2\frac{\partial\tilde{V}}{\partial r} - \frac{2}{3}\left(\frac{\partial\tilde{U}}{\partial x} + \frac{\partial\tilde{V}}{\partial r} + \frac{\tilde{V}}{r}\right) \quad (2.7)$$

$$\tilde{S}_{xx} = 2\frac{\partial\tilde{U}}{\partial x} - \frac{2}{3}\left(\frac{\partial\tilde{U}}{\partial x} + \frac{\partial\tilde{V}}{\partial r} + \frac{\tilde{V}}{r}\right) \quad (2.8)$$

$$\tilde{S}_{xr} = \tilde{S}_{rx} = \frac{\partial \tilde{U}}{\partial r} + \frac{\partial \tilde{V}}{\partial x} \quad (2.9)$$

$$\tilde{S}_{\theta\theta} = 2\frac{\tilde{V}}{r} - \frac{2}{3} \left(\frac{\partial \tilde{U}}{\partial x} + \frac{\partial \tilde{V}}{\partial r} + \frac{\tilde{V}}{r} \right) \quad (2.10)$$

Equation for the conservation of the total energy \tilde{E}

$$\begin{aligned} \frac{\partial}{\partial t} \bar{\rho} \tilde{E} + \frac{\partial}{\partial x} \left\{ \left(\bar{\rho} \tilde{E} + \bar{P} + \frac{2}{3} \bar{\rho} \tilde{k} - (\mu + \mu_t) \tilde{S}_{xx} \right) \tilde{U} \right. \\ \left. - (\mu + \mu_t) \tilde{S}_{xr} \tilde{V} - \gamma \left(\frac{\mu}{Pr} + \frac{\mu_t}{Pr_t} \right) \frac{\partial}{\partial x} \tilde{e}_i \right\} \\ + \frac{1}{r} \frac{\partial}{\partial r} r \left\{ \left(\bar{\rho} \tilde{E} + \bar{P} + \frac{2}{3} \bar{\rho} \tilde{k} - (\mu + \mu_t) \tilde{S}_{rr} \right) \tilde{V} \right. \\ \left. - (\mu + \mu_t) \tilde{S}_{xr} \tilde{U} - \gamma \left(\frac{\mu}{Pr} + \frac{\mu_t}{Pr_t} \right) \frac{\partial}{\partial r} \tilde{e}_i \right\} = 0 \end{aligned} \quad (2.11)$$

State equation for a perfect gas

$$\tilde{P} = (\gamma - 1) \bar{\rho} \tilde{e}_i \quad (2.12)$$

Where μ is the molecular viscosity, μ_t the turbulent viscosity, Pr the Prandtl number, Pr_t the turbulent Prandtl number, \tilde{e}_i the internal energy and γ the specific heat ratio.

2.3. Turbulence model

A $k - \epsilon$ model is used for the turbulence modelling. Generally, this level of closure gives good predictions for thin shear flows. The usual set of constants (Launder & Sharma 1974), "supposed universal", is not calibrated for flows where organized structures are present but for fully-developed turbulence. So, to take care of coherent unsteadiness a new calibration is necessary. The most debated constant is C_μ whose the usual value of 0.09 leans on the hypothesis of equilibrium between the sources (*Production = Dissipation*). The experimental investigation of Rodi (1972) on a round jet has shown the failure of this assumption in the near-field of this flow. This is a consequence of the organized unsteadiness which influences the energetic balance in this region. In fact, in flows where organized structures evolve, the normal stresses are larger and the turbulent shearing is weaker than in flows in equilibrium. In consequence, the basic value of C_μ is too high. Rodi (1972) had already remarked the inconstant character of C_μ and he had exprimed this quantity in function of its usual value and of the ratio between the production and the dissipation. Later, Pope (1975) proposed an effective viscosity approach for the $k - \epsilon$ model and a nonlinear function for C_μ to include some anisotropic effects. But, with these two propositions the model is then numerically more unstable. Therefore, in the present paper the value of C_μ proposed by Ha Minh & Kourta (1993) is retained. They have recalibrated this constant on a backward-facing step at a value of 0.02. The main advantage of this lower value is to imply a weaker numerical dissipation due to the lower diffusion of the model, therefore the prediction of the vortical structures is easier. A second advantage of this choice is to reduce the production of the turbulent kinetic energy generally overestimated by the $k - \epsilon$ model. There is no additive terms modelling compressibility effects in this study. According to Sarkar *et al.* (1991) the incompressible turbulence models are expected to give good results for the jets up to a Mach number of 1.5. The equations for turbulent kinetic energy and the dissipation rate can be written

under the following form:

Equation of turbulent kinetic energy

$$\frac{\partial}{\partial t} \bar{\rho} \tilde{k} + \frac{\partial}{\partial x} \left\{ \bar{\rho} \tilde{k} \tilde{U} - \mu_k \frac{\partial \tilde{k}}{\partial x} \right\} + \frac{1}{r} \frac{\partial}{\partial r} r \left\{ \bar{\rho} \tilde{k} \tilde{V} - \mu_k \frac{\partial \tilde{k}}{\partial r} \right\} = \tilde{P}_k - \bar{\rho} \tilde{\varepsilon} + W_k \quad (2.13)$$

with

$$\mu_k = \mu + \frac{\mu_t}{\sigma_k} \quad (2.14)$$

$$W_k = -2\mu\mu_t \left(\frac{\partial(\tilde{k})^{\frac{1}{2}}}{\partial x_n} \right)^2 \quad (2.15)$$

The production term expression is

$$\begin{aligned} \tilde{P}_k = & 2\mu_t \left\{ \left(\frac{\partial \tilde{U}}{\partial x} \right)^2 + \left(\frac{\partial \tilde{V}}{\partial r} \right)^2 + \left(\frac{\tilde{V}}{r} \right)^2 \right\} + \mu_t \left(\frac{\partial \tilde{U}}{\partial r} + \frac{\partial \tilde{V}}{\partial x} \right)^2 \\ & - \frac{2}{3} \left(\frac{\partial \tilde{U}}{\partial x} + \frac{\partial \tilde{V}}{\partial r} + \frac{\tilde{V}}{r} \right) \left\{ \mu_t \left(\frac{\partial \tilde{U}}{\partial x} + \frac{\partial \tilde{V}}{\partial r} + \frac{\tilde{V}}{r} \right) + \bar{\rho} \tilde{k} \right\} \end{aligned} \quad (2.16)$$

Equation for the dissipation rate of the turbulent kinetic energy

$$\begin{aligned} \frac{\partial}{\partial t} \bar{\rho} \tilde{\varepsilon} + \frac{\partial}{\partial x} \left\{ \bar{\rho} \tilde{\varepsilon} \tilde{U} - \mu_\varepsilon \frac{\partial \tilde{\varepsilon}}{\partial x} \right\} + \frac{1}{r} \frac{\partial}{\partial r} r \left\{ \bar{\rho} \tilde{\varepsilon} \tilde{V} - \mu_\varepsilon \frac{\partial \tilde{\varepsilon}}{\partial r} \right\} = \\ C_{\varepsilon_1} \tilde{P}_k - C_{\varepsilon_2} \frac{\bar{\rho} \tilde{\varepsilon}^2}{\tilde{k}} + W_\varepsilon \end{aligned} \quad (2.17)$$

with

$$\mu_\varepsilon = \mu + \frac{\mu_t}{\sigma_\varepsilon} \quad (2.18)$$

$$W_\varepsilon = \frac{-2\mu\mu_t}{\bar{\rho}} \left(\frac{\partial^2 \tilde{V}}{\partial x_n^2} \right)^2 \quad (2.19)$$

Where x_n is the distance to the wall (here x), W_k and W_ε are only active in the near wall regions, therefore in the present calculations these terms are negligible. The set of constants of the turbulence model is

$$C_\mu = 0.02; C_{\varepsilon_1} = 1.44; C_{\varepsilon_2} = 1.92; \sigma_k = 1.; \sigma_\varepsilon = 1.3 \quad (2.20)$$

3. The numerical method

3.1. The computed configuration

An air-air configuration (represented in figure 1) is predicted for several Mach numbers: a supersonic, a transonic and a subsonic (quasi-incompressible). The inlet conditions are derived from the experiment of Durão (1971) which is characterized by a lower turbulence level on the jet axis than in a fully-developed jet as the one investigated by Chassaing (1979). The different computed cases are resumed in the table 1.

The injector diameter D is 7.24 mm. The exit temperature is 300°K, the pressure

Velocity U_0 (m/s)	Mach number	Reynolds number	Inlet conditions
104	0.3	52240	Durão
333	0.96	167200	Durão
520	1.5	261200	Durão

TABLE 1. Computed cases

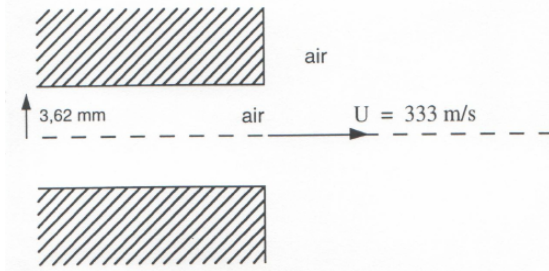


FIGURE 1. The axisymmetric configuration for the transonic jet

P_e at the exit and in the computational field is initially of 0.101 MPa and the initial density in all the field is $\rho_o = 1.28 \text{ kg}\cdot\text{m}^{-3}$. The computation used 100×93 grid points with stretching in the transverse direction outside the jet. The mesh is uniform in the x direction. The computational domain extends over 16.6 diameters in the streamwise direction and over 8.3 diameters in the transverse direction.

3.2. Numerical scheme

The numerical method used for the computations is the finite volume scheme proposed by MacCormack (1981). It is an explicit-implicit method, parabolic in time and elliptic in space. In the implicit part the treatment of viscous terms is approximated, so this algorithm is more suitable to the prediction of steady than unsteady problems. In consequence, for the present simulations only the explicit part is used in order to predict the flow instability. The equations are resolved in conservative form and the prediction-correction step procedure is utilized. This scheme is accurate to second order in time and space and does not require any additional numerical dissipation for its stability. This last skill is fundamental to the simulation of natural flow unsteadiness. Indeed, the presence of numerical dissipation would involve a large diffusion which would prevent the simulation of coherent structures. In this paper, there is no comparison of the numerical results with experiments on the mean quantities. This is due to the discrepancies between the flow pattern computed and those experimentally investigated in past studies. Nevertheless, in a previous numerical simulation (e.g. Reynier & Ha Minh 1996), a validation of our code with respect to the experimental data of Ribeiro (1972) have been led for incompressible coaxial jets.

3.3. Boundary conditions

The inlet conditions are derived from the experimental data of Durão (1971). The dissipation rate is initialized considering the flow at the inlet as a boundary layer in equilibrium. Outside the jet, a wall is present (see figure 1) in the radial direction, so Dirichlet boundary conditions (zero) are applied on this boundary for pressure and density gradients, velocity, turbulent kinetic energy and dissipation rate. The lower boundary (jet axis) is a symmetry axis so zero gradients are assumed for all quantities. For the upper boundary

two different conditions have been used: a) Neumann conditions (zero gradients) for all quantities ; b) symmetry conditions (if the flow takes place in the context of a multi-jets configuration where one jet is surrounded by several others). As the upper boundary is far from the jet interface there is no influence of this boundary condition on the flow unsteadiness. As the present study is carried out in the perspective of turbulent modelling for injection in rocket engines, the computation results presented in this paper have been obtained with symmetry conditions. The outlet conditions are deduced from characteristic relationships. They originated from the characteristic analysis theory and they have been developed for the Euler equations by Thompson (1987). These non-reflecting boundary conditions are:

$$\frac{\partial \bar{\rho}}{\partial t} - \frac{1}{c^2} \frac{\partial \bar{P}}{\partial t} = -\tilde{U} \left(\frac{\partial \bar{\rho}}{\partial x} - \frac{1}{c^2} \frac{\partial \bar{P}}{\partial x} \right) \quad (3.1)$$

$$\frac{\partial \bar{P}}{\partial t} + \bar{\rho} c \frac{\partial \tilde{U}}{\partial t} = -(\tilde{U} + c) \left(\frac{\partial \bar{P}}{\partial x} + \bar{\rho} c \frac{\partial \tilde{U}}{\partial x} \right) \quad (3.2)$$

$$\frac{\partial \tilde{V}}{\partial t} = -\tilde{U} \left(\frac{\partial \tilde{V}}{\partial x} \right) \quad (3.3)$$

$$\frac{\partial \bar{P}}{\partial t} - \bar{\rho} c \frac{\partial \tilde{U}}{\partial t} = -(\tilde{U} - c) \left(\frac{\partial \bar{P}}{\partial x} - \bar{\rho} c \frac{\partial \tilde{U}}{\partial x} \right) \quad (3.4)$$

When the flow is subsonic the pressure must be specified at the exit, a zero gradient is applied for this quantity. For the turbulent kinetic energy and its dissipation rate the same conditions are used on this boundary.

4. Results

Section § 4.1 focuses on presence of instabilities and evolution of the coherent structures in the near-field of the jet. The evolution of flow quantities (velocity, pressure, density, turbulent kinetic energy and dissipation rate) in the flow-field and their interaction with the organized unsteadiness are presented in § 4.2. The compressibility effects and their influence on large scale structures are studied in section § 4.3. A comparison between the Strouhal numbers obtained experimentally and our numerical results is shown in this last section.

4.1. The unsteady round jet

4.1.1. Presence of unsteadiness

The executed computations with inlet conditions derived from the experimental data of Durão (1971) lead to the simulation of instabilities (see figure 2) in the near-field without any flow excitation. The figure 2 represents the time-dependent variations of the streamwise velocity for a point located in the shear-layer at $x=1.5D$ and $y=0.5D$. This quasi-periodic phenomenon is independent from the Mach number. If for a Mach number of 0.3 the variations are quasi-sinusoidal, this is not the case for the transonic and supersonic jets, due to the presence of a pairing near this location. The corresponding spectra obtained by Fourier analysis over one hundred periods are presented in figure 3. They show a dominant frequency for the unsteadiness and some harmonics for the two higher Mach numbers. The dominant frequency is equal to 5600 Hz for the quasi-incompressible case, 17500 Hz for the transonic jet and 23800 Hz for the supersonic

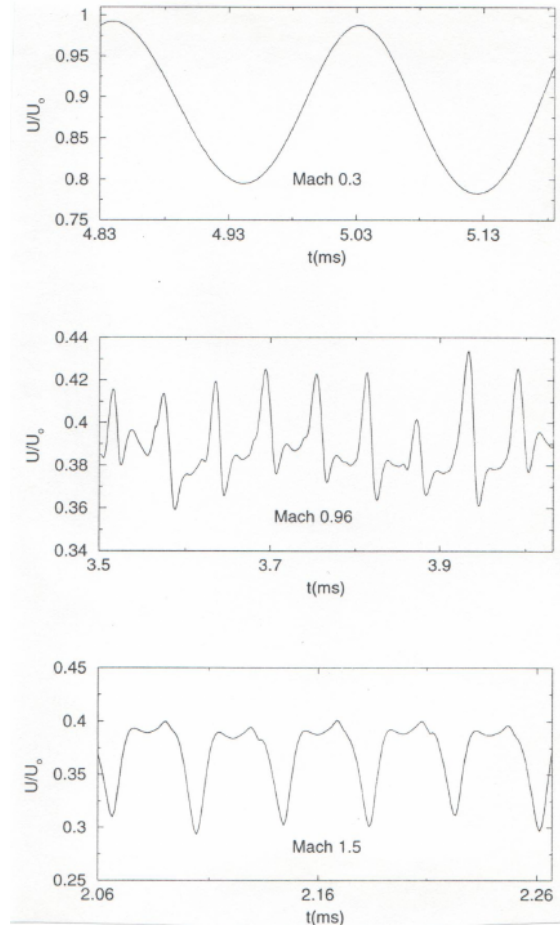


FIGURE 2. Time-variations of the streamwise velocity in the near-field at $x=1.5D$ and $y=0.5D$:
 a) Mach 0.3; b) Mach 0.96; c) Mach 1.5

jet. These instabilities correspond to the dominant large scale structure evolving in the mixing layer. The associated Strouhal numbers (calculate from the diameter of the inlet pipe and the exit velocity) are 0.39 for a Mach number of 0.3, 0.38 for the transonic jet and 0.33 for the supersonic jet. The Strouhal numbers are in the range of values contained between 0.3 and 0.4 corresponding to the preferred mode observed in the experiments of Crow & Champagne (1971) and Hussain & Zaman (1981), and predicted by the theory (e.g. Michalke 1984). This preferred mode corresponds to the coherent structures which dominate the shear-layer of a round jet.

4.1.2. Coherent structure evolution

The unsteady profiles of velocity, pressure, density, turbulent energy and dissipation rate of turbulent energy are fitted in figures 4 to 9. These figures show the unsteady variations for four sections of the mesh located at $x=0.33D$, $x=2D$, $x=5D$ and $x=15D$, for four moments of a pseudo-period: $T/4$, $T/2$, $3T/4$ and T . A high unsteadiness is active for all quantities in the near region at $x=0.33D$ and $x=2D$. This flow unsteadiness originates from the fluctuations in the shear-layer of the jet. The mixing layer becomes unstable near the inlet, due to the Kelvin-Helmholtz instability, then rolls up to form vortex rings.

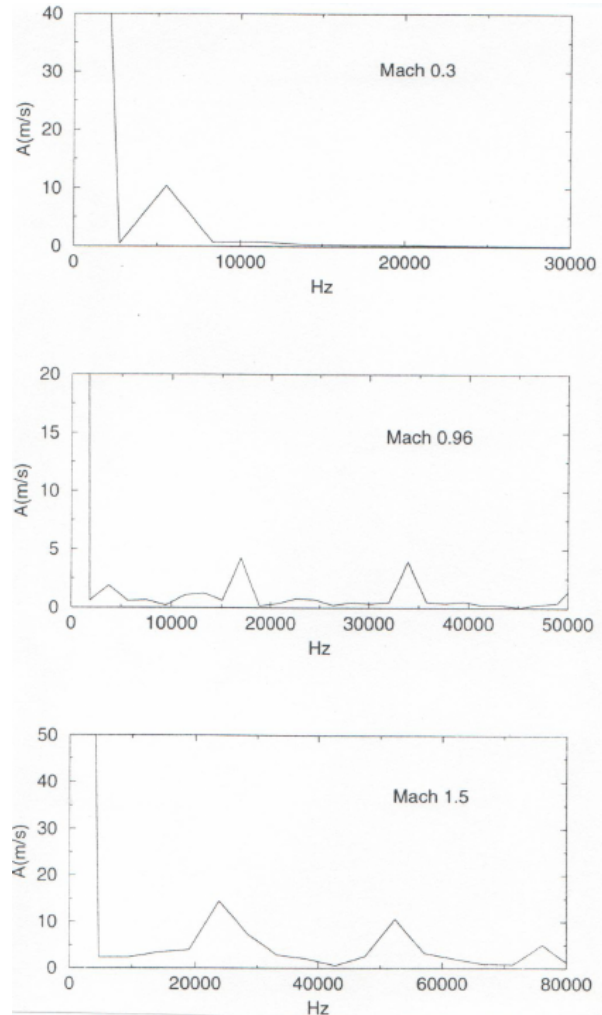


FIGURE 3. Spectra of time-variations of the streamwise velocity in the near-field at $x=1.5D$ and $y=0.5D$: a) Mach 0.3; b) Mach 0.96; c) Mach 1.5

This phenomenon has been largely experimentally studied by Liepmann & Gharib (1992) and numerically by Verzicco & Orlandi (1994) for the incompressible jet. In the present calculations the coherent structures appear very close to the inlet. The numerical results put in evidence a strong flow instability for $x=0.33D$ and $x=2D$. They are in agreement with the experiments of Arnette *et al.* (1993) and Liepmann & Gharib (1992) and the numerical study of Grinstein *et al.* (1987) which report the presence of instabilities before two diameters. After this location, the vortical structures grow by pairing. Grinstein *et al.* (1987) simulated several pairings in the near-field of a compressible jet. They showed that pairings occur at determined locations in the flow, when the resulting vortice is too large the potential core is broken up. This process is fundamentally different in the round jet compared to the plane jet. As shown in figures 10 and 11, it involves the contraction and the expansion of the vortice rings and affects the potential core (see also figures 4 to 9) by the induction phenomenon of Biot and Savart. The evolution of the coherent structures is largely influenced by this process of contraction and shearing which involves the

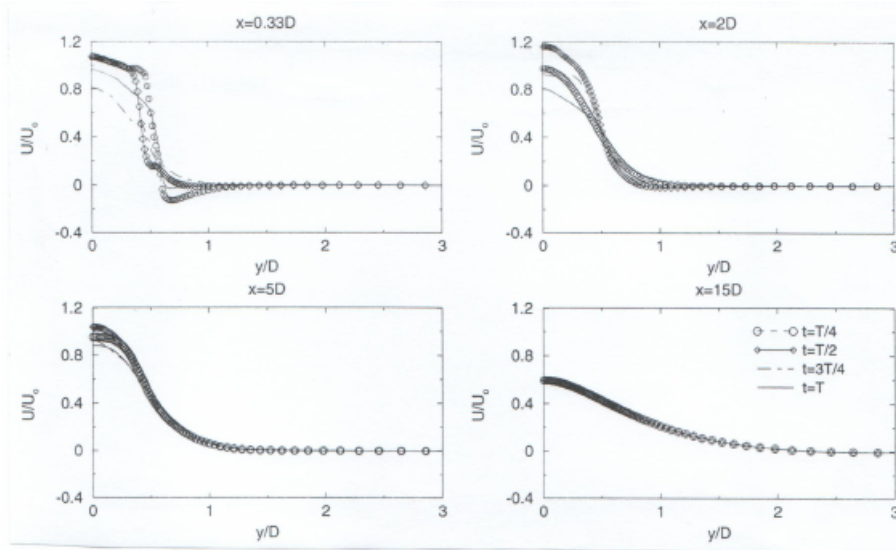


FIGURE 4. Profiles of the unsteady streamwise velocity for the transonic jet

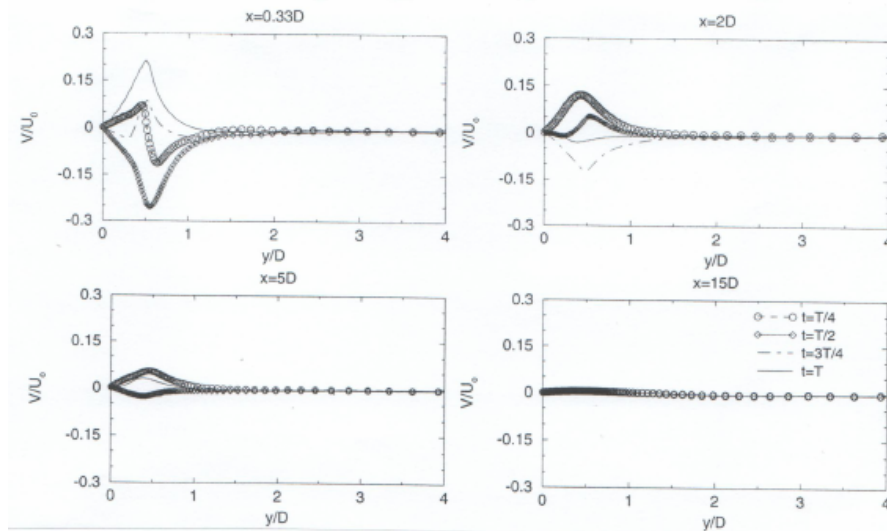


FIGURE 5. Profiles of the unsteady radial velocity for the transonic jet

distorsion of the vortical structures (Fourguette *et al.* 1991). Moreover, this mechanism accelerates the evolution of the secondary three-dimensional structures as demonstrated by Liepmann & Gharib (1992). The present results put in evidence the damping of the coherent structures as they are convected downstream (figures 4 to 9). The figure 11, where the field of the unsteady radial velocity is visualized, shows clearly this decay of the large scale structures. The unsteadiness is strong at $x=0.33D$ and $x=2D$ (see figures 4 to 9), downstream at $x=5D$ the coherent structures are weakened and at $x=15D$ the flow has a steady aspect. The weakening of the unsteadiness in the near-field corresponds to the transfer of a substantial part of the coherent instability to random turbulence. So, the decay of coherent structures is correlated by the turbulence development. Near the inlet at $x=0.33D$ the turbulent quantities (figures 8 and 9) are strongly unsteady and

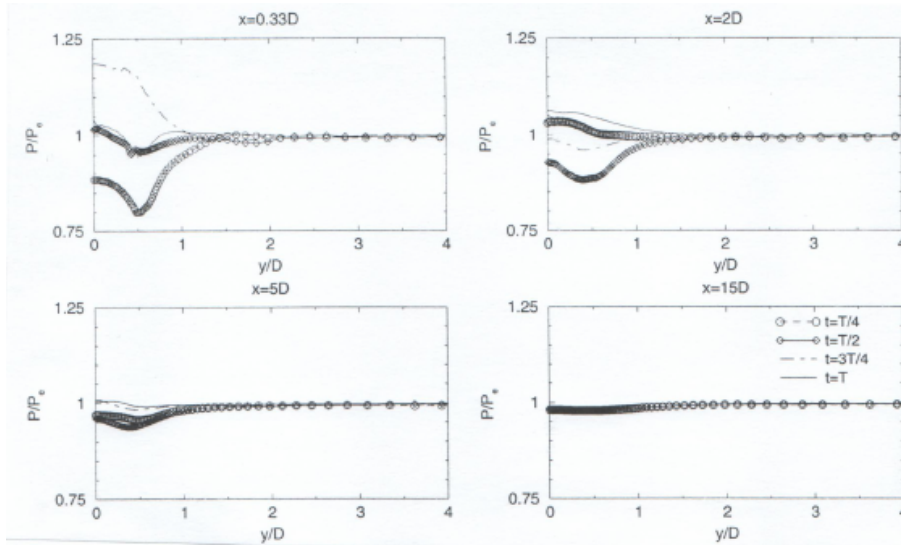


FIGURE 6. Profiles of the unsteady pressure for the transonic jet

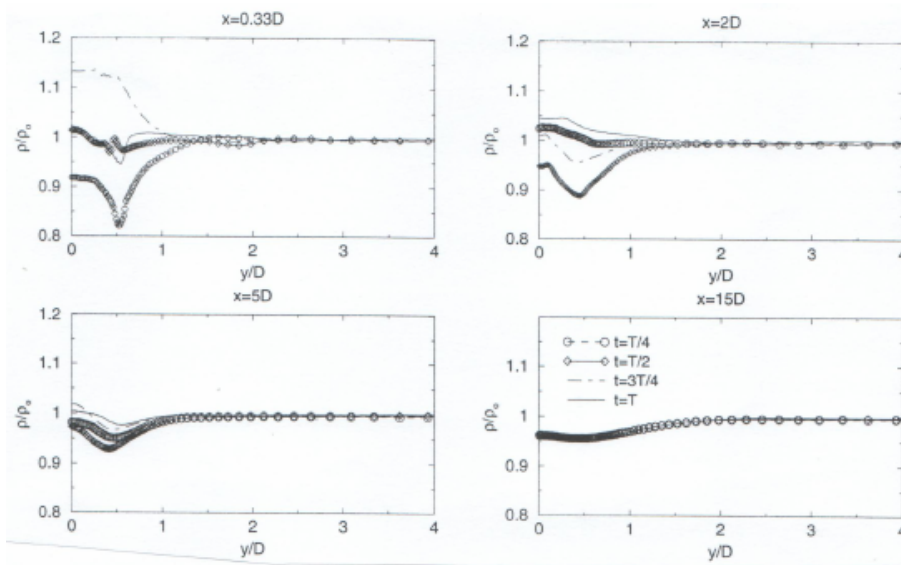


FIGURE 7. Profiles of the unsteady density for the transonic jet

the time-averaged level (see figure 16) is low. This corresponds to a domination of the coherent structures. Downstream at $x=2D$ and $x=5D$, the large scale structure dominance shades off and the coherent part becomes of the same order then weaker than the random component. The damping of the organized unsteadiness is due to the nonlinear effects. They are generated by the growth of the Kelvin-Helmholtz instability waves, they involve a swifter diffusion of the mean flow and the generation of random turbulence by the Reynolds stresses. This evolution of the two-dimensional structures is in agreement with the experimental investigation of Sokolov *et al.* (1981). These authors observed the same features in the evolution of coherent structures in the near-field of a round jet. Moreover, they demonstrated that at $x/D=1.5$ the structure front is characterized by an

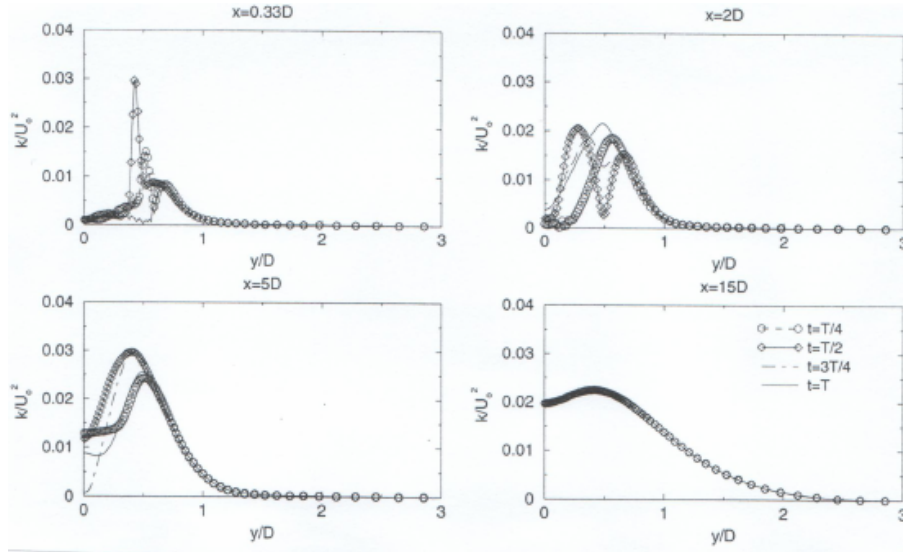
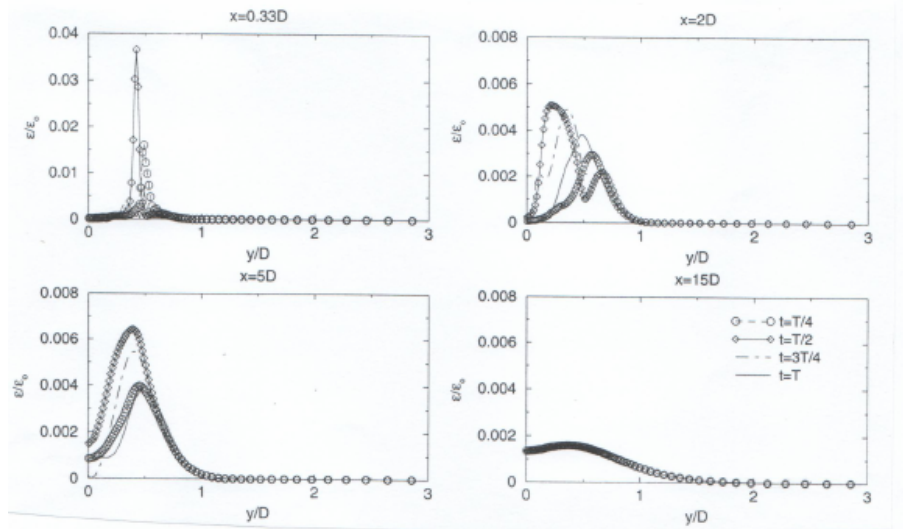


FIGURE 8. Profiles of the unsteady turbulent kinetic energy for the transonic jet

FIGURE 9. Profiles of the unsteady dissipation rate for the transonic jet (with $\epsilon_o = U_o^3/D$)

intense shearing when the drag is a diffusive zone. Downstream, at $x/D=4.5$, the shearing is weakened by the action of the diffusion mechanisms. In this experiment, up to $x/D=4.5$ the coherent turbulence is gradually diluted but at this location this quantity is larger than the random turbulence. According to these authors, at the end of the potential core located at four or five diameters the instability waves reached an adequate magnitude to influence the flow. Then the shear-layer and the jet width grow fastly. The visualization of the unsteady field of the radial velocity for the supersonic jet in figure 11 shows the vanishing of the coherent structures before eleven diameters. This result is close to the experimental observations of Hussain & Zaman (1981) who show that the periodicity of the large scale vortices is lost beyond $x=8D$. Liepmann & Gharib (1992) locate this region at $x=10D$ where the round jet lost its organized aspect. These discrepancies in

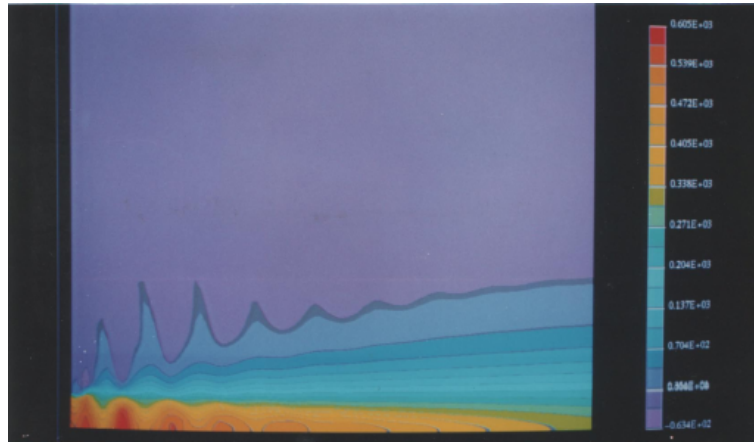


FIGURE 10. Field of the unsteady streamwise velocity for the supersonic jet

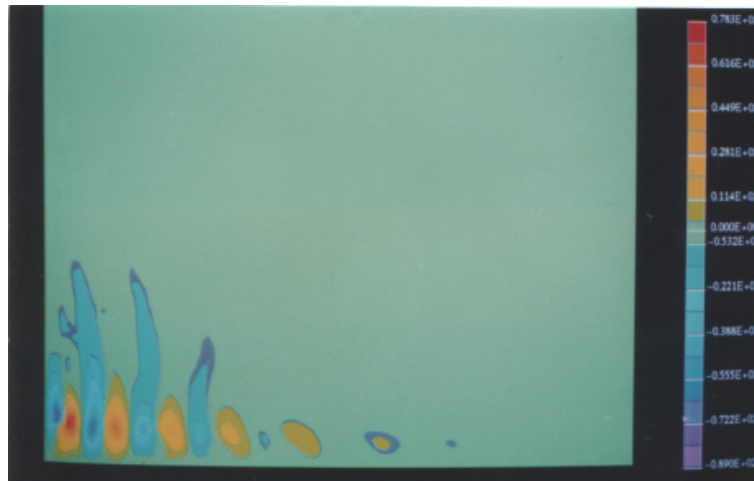


FIGURE 11. Field of the unsteady radial velocity for the supersonic jet

the exact location of the coherent structure vanishing may be explained by different inlet conditions.

4.2. Flow quantities and interaction with coherent structures

4.2.1. Coherent structures and velocity field

The profiles of streamwise and radial unsteady velocities (figures 4 and 5) show a high instability near the inlet at $x=0.33D$ and $x=2D$. The visualization of the unsteady field of the spanwise velocity in figure 11 puts in evidence an alley of vortices moving in the mixing layer already experimentally observed by Lau & Fisher (1975). These structures decay as they move downstream and they disappear in the far-field after eleven diameters. The field of the unsteady streamwise velocity (see figure 10) allows the observation of expansion and contraction process of the vortice rings. These last ones, located in the mixing layer, affect the central zone by the induction phenomenon of Biot and Savart. The central region is then characterized by a succession of regions of compression and expansion. Downstream, at $x=5D$ and $x=15D$ (see figures 4 and 5),

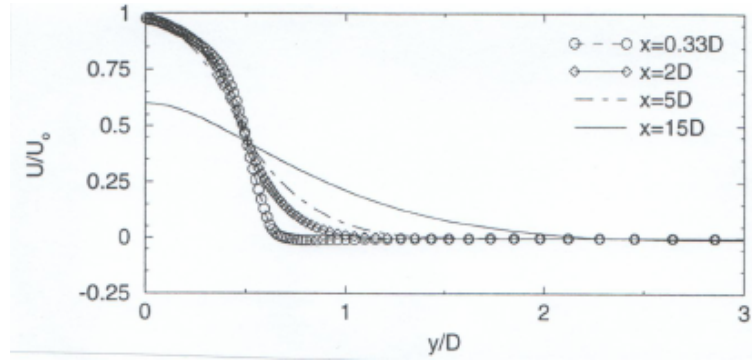


FIGURE 12. Profiles of time-averaged streamwise velocity for the transonic jet

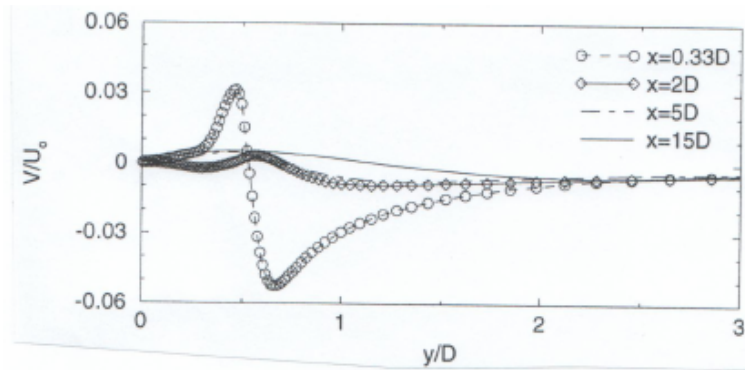


FIGURE 13. Profiles of time-averaged radial velocity for the transonic jet

the velocity unsteadiness damps and the flow becomes more diffusive which involves the velocity decrease and the jet expansion (see figure 12).

The profiles of unsteady and time-averaged (figures 5 and 13) radial velocities put in evidence the high level of the radial velocity in the near region. Its intensity decreases downstream at $x=5D$ and $x=15D$. The maximum near the inlet proves the high entrainment in the near-field. The experimental investigation of Hussain & Zaman (1981) confirms the strong entrainment in this region. They located the maximum of the spanwise velocity between 3.5 and 8 diameters, whereas in our results it takes place nearer the inlet. This high entrainment has been also observed by Liepmann & Gharib (1992) who established the link with the presence of coherent structures. In fact, more the jet is laminar, more it is apt to imply a high entrainment. In this flow, the coherent structures evolving in the mixing layer influence drastically the entrainment process which rises under their effects.

4.2.2. Interaction with thermodynamic quantities

A high unsteadiness of the pressure can be seen in the near-field at $x=0.34D$ and $x=2D$ (see figure 6). According to Zhou & Lin (1992) these pressure fluctuations are at the source of the instability waves which involve the genesis of the coherent structures. The analysis of the time-averaged pressure profiles (figure 14) shows a minimum in the mixing layer whereas a maximum is located in the central region on the axis. This fact has been already reported by Grinstein *et al.* (1987) in a numerical investigation. According to these authors the pressure minima coincide with the minima of the normal stress in the

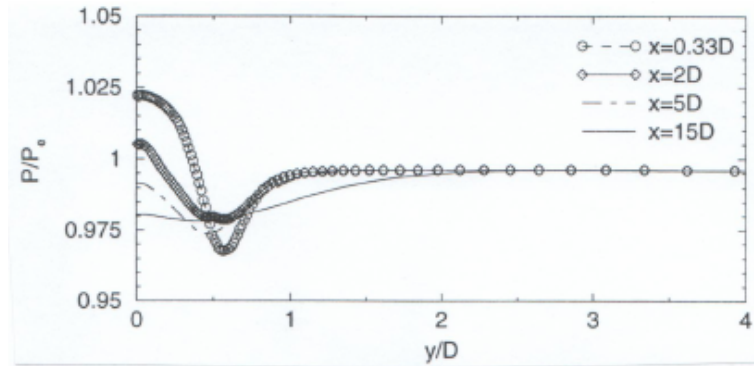


FIGURE 14. Profiles of the time-averaged pressure for the transonic jet

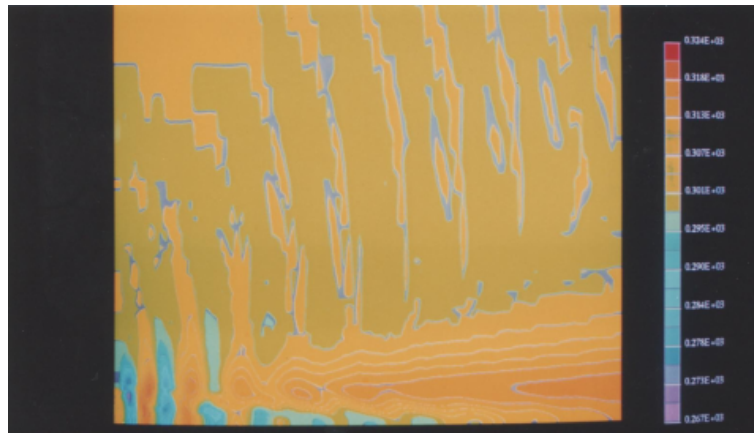


FIGURE 15. Field of the unsteady temperature for the supersonic jet

radial direction. This points out the determinant role of the spanwise velocity fluctuations in the generation of the static pressure decrease from the axis until the mixing layer. At this location the pressure is generally weaker than the ambient pressure, while a local maximum is located in the potential core where the vortices are away. This pressure discrepancy between the shear-layer and the potential core is due to velocity gradients. According to Batchelor (1967) the variation of the time-averaged pressure compared to the pressure at the equilibrium is function of the velocity gradient. The succession of minima and maxima of the unsteady pressure in the mixing layer is a consequence of the interaction between the pressure field and the coherent unsteadiness. The minima correspond to the vortical structure centres and the maxima are located between the vortices (Hussain 1986).

The density (see figure 7) presents the same tendencies that the pressure in the near-field. A local maximum is situated in the central region while the minimum is reached in the shear-layer. The high unsteadiness near the inlet damps downstream. When the coherent structures have disappeared after $x/D=11$, the turbulent flow is almost fully-developed. Then the diffusion effects rise and the density becomes uniform at the level of the surrounding density.

The field of the unsteady temperature (see figure 15) shows clearly the variations of this quantity in the mixing layer at the time of the vortice crossing. The temperature increases in the far-field after eleven diameters, this corresponds to the progressive degradation of

the energy contained in the jet by the dissipative mechanisms associated to the mean and turbulent motions.

Finally, a high influence is found in the near-field between the evolution of the thermodynamic quantities and the evolution of the organized structures. This fact puts in evidence the coupling between these quantities and the coherent part of the turbulence.

4.2.3. Turbulent field

The analysis of the turbulent field (figures 8 and 9) clues that the shear-layer is a region where a high level of turbulence occurs. Indeed, the turbulence is generated in this zone where the shearing is intense. As for the other quantities (velocity, density and pressure) the variations of turbulent energy and of dissipation rate are very large in the near-field and disappear progressively downstream. This high unsteadiness is associated with the presence of coherent structures. The regions located between the large scale vortices are characterized by a strong shearing, so the maxima of the turbulent energy occur in these zones. This result is in agreement with the theory on coherent structures developed by Hussain (1983, 1986). Near the inlet, at $x=0.33D$ (figure 8), compared to the time-averaged quantities (figure 16), the amplitude of the unsteadiness is very high: more than three times the time-averaged turbulent energy for the transonic jet. This fact is in agreement with the experiments of Hussain & Zaman (1981) and Sokolov *et al.* (1981) where the coherent part of the turbulent energy is much greater than the random part in the near-field. This indicates a domination of the large scale vortices with respect to the small scale turbulence. Between $x=0.33D$ and $x=5D$ (see figures 8 and 9) the organized unsteadiness decays significantly, the coherent structures damp as they are convected downstream. The weakening of the large scale vortices is correlated by an increase of the time-averaged turbulent energy (see figure 16) between these two locations. The growth of the incoherent turbulence is due to the transfer of a substantial part of the organized instability to random turbulence by the nonlinear mechanisms of the flow. After $x=5D$ the unsteadiness is weak so the turbulence is dominated by the small scales. The residual instability has disappeared at eleven diameters.

On the modelling aspect, the unsteadiness simulated in the near-field of the compressible round jet supports that the equality supposed between the production and the dissipation which is at the source of the classical modelling is not verified in the whole jet. If this hypothesis is valid in the fully-developed region of a round jet, this is not the case in the near-field as shown by Rodi (1972) in an experimental investigation. The presence of coherent structures alters strongly the near-field. The energy spectra is not equilibrated in this region due to the presence of peaks (e.g. Ha Minh & Kourta, 1993) which correspond to the coherent structures.

The mean level of the turbulent kinetic energy is low in the near-field (figure 16) especially in the central region. In this zone the velocity gradients are weak, a low production is involved which explains the central depression predicted in the turbulent energy profiles. The turbulent energy is produced in the mixing layer where a high shearing occurs between the vortices. This agrees with the experimental results of Panchapakesan & Lumley (1993) where the production is in majority some shear production. The presence of a central depression has also been observed by Bogulawski & Popiel (1979). In the present simulations the depression is progressively filled downstream by the extension of the mixing layer and the resulting diffusion. The turbulent energy maximum has been located in the mixing layer between $2.5D$ and $7D$ by Hussain & Zaman (1981) and at about $6D$ by Bogulawski & Popiel (1979). In the present study the maximum occurs at $9.5D$ for the subsonic flow (Mach 0.3). In fact, the location of the maximum depends on both inlet conditions and Reynolds number according to Bogulawski & Popiel (1979).

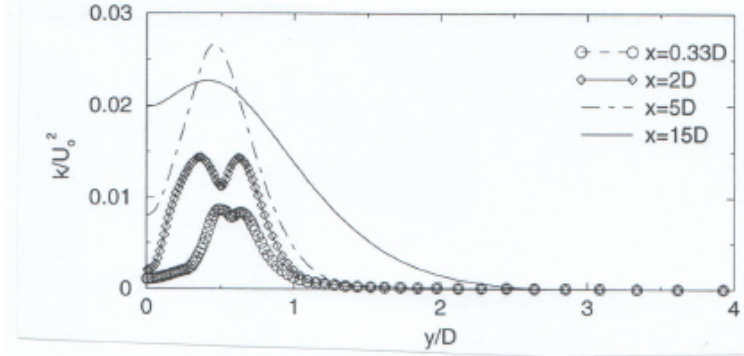


FIGURE 16. Profiles of the time-averaged turbulent energy for the transonic jet

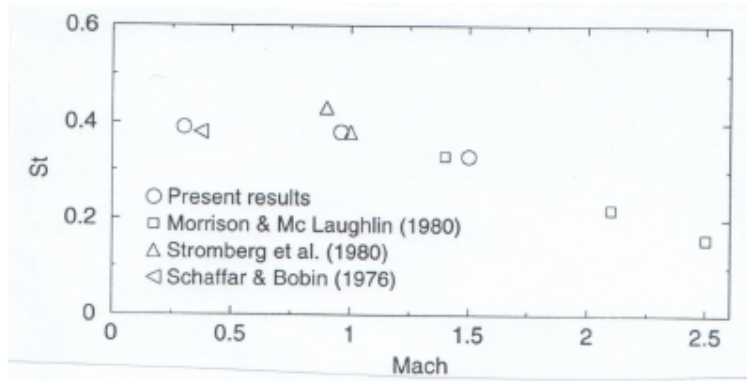


FIGURE 17. Evolution of the Strouhal number with the Mach number

4.3. Compressibility effects

4.3.1. On preferred mode

Flow computations for Mach numbers of 0.3, 0.96 (see figures 4 to 9) and 1.5 show the near-field domination by the organized unsteadiness (e.g. Reynier 1995). These instabilities are quasi-periodic (see figure 2) and square with the preferred mode found by Crow & Champagne (1971). The present results on near-field vortices allow the evaluation of the Mach number influence on the Strouhal number associated to the dominant instability. The figure 17 represents the Strouhal numbers measured by Schaffar & Bobin (1976), Stromberg, McLaughlin & Troutt (1980) and Morrison & McLaughlin (1980) and the present computation results. There is an excellent agreement between our numerical predictions and the values provide by experiments for the transonic and supersonic jets. The value predicted for the quasi-incompressible jet is very close to that of 0.38 measured by Schaffar & Bobin (1976) for an exit velocity of 130m/s. For the simulations with the Mach numbers of 0.3 and 0.96 the Strouhal number stays quasi-firm. For this velocity range, the compressibility effects remain weak and the turbulence structure is not fundamentally altered. It is not the same for the supersonic jet where the convective Mach number is larger. In our calculations the Strouhal number of the dominant component decays when the Mach number increases (its value is 0.38 for Mach 0.96 and 0.33 for Mach 1.5). This agrees with the experimental investigations of Lepicovski *et al.* (1987) and Morrison & McLaughlin (1980). The Strouhal number decrease with the Mach number growth is to put together with the theory of Papamoschou & Roshko (1988) on compressible mixing

Mach number	Time-variation $\frac{\Delta \bar{p}}{\rho_0}$	Time-variation $\frac{\Delta \bar{k}}{U_0^2}$	Time-variation $\frac{\Delta \bar{v}}{U_0}$
0.3	0.018	0.016	0.35
0.96	0.18	0.02	0.317
1.5	0.38	0.0195	0.256

TABLE 2. Maximum time-variations of several flow quantities in the mixing layer at $x=1.5D$ and $y=0.53D$

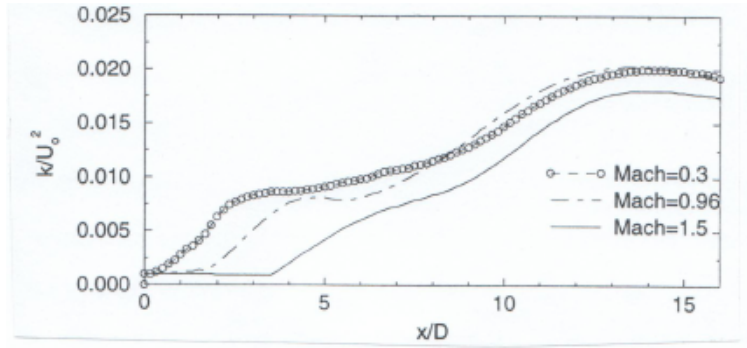


FIGURE 18. Axis evolution of the time-averaged turbulent energy for the three computed cases

layers. The decrease of the Strouhal number corresponds to a diminution of the number of coherent structures evolving in the jet. This places in a prominent position the stabilizing effect of the Mach number on the flow. The diminution of the dominant mode of the Strouhal number for the compressible flows is caused, according to Miles (1958), by a decrease of the growth rate of the Kelvin-Helmholtz instability.

4.3.2. On turbulence and coherent structures

In table 2, the maximum adimensional time-fluctuations of density, turbulent energy and radial velocity are compared for the three computed cases at $x=1.5D$ and $y=0.53D$. The table shows a growth of the time-fluctuations for the density with the Mach number. This seems logical because the compressibility effects are more important for the transonic and supersonic jets. The adimensional time-variations decrease for the radial velocity with the Mach number but the absolute variations rise. For the turbulent kinetic energy the adimensional time-fluctuation is quasi-firm. This shows a growth of the absolute fluctuations with the square of the Mach number. This indicates a dependence of the coherent structure characteristics on the Mach number. Arnette *et al.* (1993) also observed the increase in strength of the large scale vortices with the Mach number. In their experimental investigation on a compressible round jet Hussain & Zaman (1981) established that the large scale structures depend on the Reynolds number. By splitting the Reynolds stresses in two components, Hussain & Zaman (1981) pointed out that the coherent part of the turbulence becomes larger for high Reynolds numbers. They also remarked that the coherent structures become more energetic. The momentum transport across the shear-layer is then larger: this agrees with the increase of turbulent energy and radial velocity time-variations for the high Mach numbers in the present numerical simulations.

The evolution of the time-averaged turbulent energy on the axis for the different simulations is plotted in figure 18. The axis profiles of the turbulent energy level off in the near-field which corresponds to the potential core region. The plateau where the turbu-

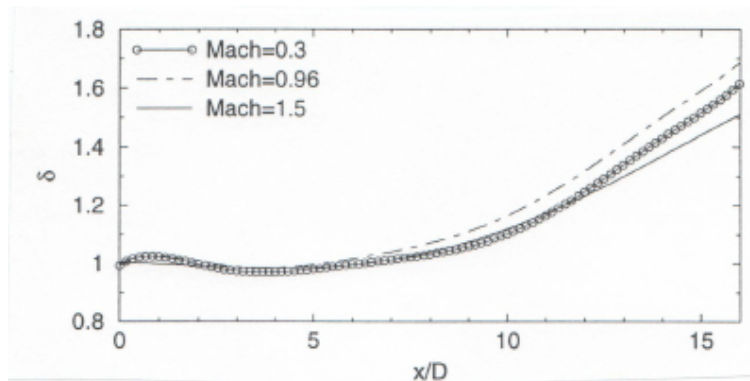


FIGURE 19. Evolution of the expansion rate with the Mach number

lent energy is low is due to a weak production in the central region of the jet. The length of the plateau rises with the Mach number. Morrison & McLaughlin (1980) observed in their experiment on supersonic jets the dependence of the potential core length on both Mach and Reynolds numbers. Its length increases with the first and decreases with the second. The first point is well correlated by our numerical results. Downstream the region where the turbulent energy levels off, the curves show a strong growth of the turbulent energy. This is a consequence of the transfer of a coherent turbulence substantial part to random turbulence. This shows, in agreement with Sokolov *et al.* (1981), that the end of the potential core is characterized by a drastic change in the turbulence structure. The increase of the turbulent energy originates from the growing of the mixing layer which involves the diffusion of the turbulence from this region to the whole jet. After 10D the turbulent energy (see figure 18) follows the same evolution for the three computed cases, the compressibility effects are attenuated in this region of the flow where the coherent structures have vanished (see § 4.1.2).

4.3.3. Influence on expansion rate

In figure 19 the expansion rates computed for the three Mach numbers are represented. If the Mach number has a stabilizing effect on the flow, the expansion rate should decrease when the Mach number increases. Paradoxically, the jet has a greater expansion at Mach 0.96 than at Mach 0.3, whereas the expansion rate is lower for the supersonic case. The compressibility effects are weak for the low values of the convective Mach, then the growth rate of the Kelvin-Helmholtz instability has not been largely reduced between Mach numbers of 0.3 and 0.96. But the Reynolds number has slightly increased which explains the expansion rate growth. This phenomenon is directly linked to the characteristics of the coherent structures. According to Hussain & Zaman (1981) they depend on the Reynolds number. The momentum transport across the shear-layer is greater at high Reynolds numbers: this implies a rise of diffusion and expansion rate. In the present predictions the Strouhal number is quasi-firm between the Mach numbers of 0.3 and 0.96. This indicates that the same number of coherent structures evolves in the near-field. But, the Reynolds number has increased so the diffusion is more important which explains the higher expansion rate for the jet at Mach 0.96.

In agreement with the survey of the jet instability theory by Michalke (1984), the expansion rate is weaker for the supersonic jet. This is a consequence of the Strouhal number diminution (see figure 17). Indeed, the presence of coherent structures has for effect an increase of the flow interface, when the Strouhal number reduces, the interface

length becomes shorter and the diffusion in the flow is weaker. This point explains the reduction of the expansion rate for the supersonic jet in our simulations. As in the paragraph § 4.3.1 where the Mach number effect implies a Strouhal number decrease, the diminution of the expansion rate for the supersonic jet shows a stabilization of the jet by the compressibility effects. This agrees as previously with the theory of Papamoschou & Roshko (1988). The lessening of the expansion rate for the supersonic Mach numbers has been already experimentally investigated in coaxial jets by Schadow, Gutmark & Wilson (1989) who have established the dependence of the expansion rate on the convective Mach number.

5. Conclusion

The results presented in this paper have been obtained for compressible jets with an under-developed turbulence at the inlet. In this compressible flow, the use of the semi-deterministic modelling allows the simulation of the unsteadiness corresponding to the coherent structures which evolve in the near-field and dominate the mixing layer of the jet. The agreement between the Strouhal numbers of the preferred mode corresponding to the dominant instability predicted by the calculations for several Mach numbers and those provided by previous experiments is excellent. Moreover, the evolution of the large scale vortices and their interaction with the unsteady fields of velocity, pressure and turbulent quantities predicted by the simulations show the same features than in previous experiments. The instability appears very close to the inlet, the unsteadiness is strong at $x=0.33D$, and decays by moving downstream. The coherent structures vanish at eleven diameters which agrees with other experimental investigations. The profiles of the time-averaged pressure show its decrease from the axis until the mixing layer. The pressure variations in the mixing layer at the time of the coherent structure crossing have been also simulated. These results agree with previous numerical simulations and theory on coherent structures. The unsteadiness of the turbulent quantities shows a strong coupling with the evolution of the large scale vortices. The coherent turbulence dominating the near-field is transferred to random turbulence under the action of the nonlinear mechanisms of the flow. In consequence, the growth of the random turbulence is correlated by the damping of the coherent structures.

The results on the influence of compressibility effects on dominant instability and expansion rate are in agreement with previous theory on the stabilization of flows by the Mach number increase. The Strouhal number of the preferred mode reduces with the Mach number growth. The expansion rate depends on the coherent structures, it rises with the Reynolds number and decreases with the Mach number for the supersonic jet. The large scale vortices become more energetic for high Mach numbers but they are more rarely which explains the decrease of the expansion rate.

If this study is proving conclusive, some improvements of the method applied here are possible. The prediction of the location of the turbulent energy maximum in the jet is not in fair agreement with experiments. If the inlet conditions are not the same this cannot absolutely justify this discrepancy. In the model used, the constants have been recalibrated on a backward-facing step and not on a jet. To escape of a new calibration for every flow, a solution is to use functions at the place of constants to take account of the organized unsteadiness. This involves a turbulence model more nonlinear, therefore a numerical scheme more unstable. Another solution would be the use of a model more elaborated as a Reynolds stress model to improve the result precision. Therefore, the method applied in this paper allows the best hopes to the simulation of coherent structures for flows at high Reynolds numbers and constitutes an alternative to the LES.

Financial support for this study was provided by the Société Européenne de Propulsion under contract PRC/CNRS n°90.0018C. We are also grateful to the CNES which supports this work under the post doctorate grant of P. Reynier.

REFERENCES

- ARNETTE, S. A., SAMIMY, M. & ELLIOT, G. S. 1993 On streamwise vortices in high Reynolds number supersonic axisymmetric jets. *Phys. Fluids A* **5**, 187–202.
- BATCHELOR, G. K. 1967 *An introduction to fluid dynamics*. Cambridge University Press.
- BOGULAWSKI, L. & POPIEL, CZ. O. 1979 Flow structure of the free round turbulent jet in the initial region. *J. Fluid Mech.* **90**, 531–539.
- BROWN, G. L. & ROSHKO, A. 1974 On density effects and large structure in turbulent mixing layers. *J. Fluid Mech.* **64**, 775–816.
- CHASSAING, P. 1979 Mélange turbulent de gaz inertes dans un jet de tube libre. Ph. D. thesis, INPT n°42, Toulouse.
- CLEMENS, N. T. & MUNGAL, M. G. 1992 Two and three dimensional effects in supersonic mixing layer. *AIAA J.* **30**, 973–981.
- CROW, S. C. & CHAMPAGNE, F. H. 1971 Orderly structure in jet turbulence. *J. Fluid Mech.* **48**, 547–591.
- DURÃO, D. 1971 Turbulent mixing of coaxial jets. Mast. of Science thesis, Imperial College of Science and Technology, London.
- FAVRE, A. 1965 Equations des gaz turbulents compressibles. *J. de Mécanique* **4**, 361–390 and 391–421.
- FOURGUETTE, D. C., MUNGAL, M. G. & DIBBLE, R. W. 1991 Time evolution of the shear-layer of supersonic axisymmetric jet. *AIAA J.* **29**, 1123–1130.
- GRINSTEIN, F. F., ORAN, E. S. & HUSSAIN, A. K. M. F. 1987 Simulation of the transition region of axisymmetric free jets. *6th Symp. Turb. Shear Flows*, Toulouse.
- HA MINH, H. & KOURTA, A. 1993 Semi-deterministic turbulence modelling for flows dominated by strong organized structures. *9th Symp. Turb. Shear Flows*, Kyoto.
- HUSSAIN, A. K. M. F. 1983 Coherent structures—reality and myth. *Phys. Fluids A* **26**, 2816–2850.
- HUSSAIN, A. K. M. F. 1986 Coherent structures and turbulence. *J. Fluid Mech.* **173**, 303–356.
- HUSSAIN, A. K. M. F. & ZAMAN, K. B. M. Q. 1981 The preferred mode of the axisymmetric jet. *J. Fluid Mech.* **110**, 39–71.
- LAU, J. C. & FISHER, M. J. 1975 The vortex street structure of turbulent jets. Part 1. *J. Fluid Mech.* **67**, 299–337.
- LAUNDER, B. E. & SHARMA, B. I. 1974 Application of the energy dissipation model of turbulence to the calculation of flow near a spinning disc. *Lett. Heat Mass Transfer* **1**, 131–138.
- LEPICOVSKI, J., AHUJA, K. K., BROWN, W. H. & BURRIN, R. H. 1987 Coherent large scale structures in high Reynolds number supersonic jets. *AIAA J.* **25**, 1419–1425.
- LIEPMANN, D. & GHARIB, M. 1992 The role of streamwise vorticity in the near field entrainment of round jets. *J. Fluid Mech.* **245**, 643–668.
- MACCORMACK, R.W. 1981 A numerical method for solving the equations of compressible viscous flow. *AIAA Paper*, 81-0110.
- MICHALKE, A. 1984 Survey on jet instability theory. *Prog. Aerospace Sci.* **21**, 159–199.
- MILES, J. W. 1958 On the disturbed motion of a plane vortex sheet. *J. Fluid Mech.* **4**, 538–552.
- MOORE, C. J. 1977 The role of shear-layer instability waves in jet exhaust noise. *J. Fluid Mech.* **80**, 321–367.
- MORRISON, G. L. & MCLAUGHLIN, D. K. 1980 Instability process in low Reynolds supersonic jets. *AIAA J.* **18**, 793–800.
- OERTEL, H. 1982 Coherent structures producing Mach waves inside and outside of the supersonic jet. Structure of complex turbulent shear flow. *IUTAM Symp.*, Marseille.
- PANCHAPAKESAN, N. R. & LUMLEY, J. L. 1993 Turbulence measurements in axisymmetric jets of air and helium. Part 1 : Air jet. *J. Fluid Mech.* **246**, 197–223.

- PAPAMOSCHOU, D. & ROSHKO, A. 1988 The compressible turbulent shear-layer: an experimental study. *J. Fluid Mech.* **197**, 453–477.
- POPE, S. B. 1975 A more general effective-viscosity hypothesis. *J. Fluid Mech.* **72**, 331–340.
- RAGAB, S. A. & WU, J. L. 1989 Linear instabilities in two-dimensional compressible mixing layers. *Phys. Fluids A* **1**, 957–966.
- RAYLEIGH, LORD 1879 On the instability of jets. *Proc. London Math. Soc.* **10**, 4–13.
- REYNIER, P. 1995 Analyse physique, modélisation et simulation numérique des jets simples et des jets coaxiaux turbulents, compressibles et instationnaires. Ph. D. thesis, INPT n°1062, Toulouse.
- REYNIER, P. & HA MINH, H. 1995 Influence of density contrast and compressibility on instability and mixing in coaxial jets. *10th Symp. Turb. Shear Flows*, Penn. State University.
- REYNIER, P. & HA MINH, H. 1996 Numerical prediction of unsteady compressible turbulent coaxial jets. *Computers and Fluids*, accepted.
- REYNOLDS, W. C. & HUSSAIN, A. K. M. F. 1972 The mechanics of an organized wave in turbulent shear flow. Part 3: Theoretical models and comparison with experiments. *J. Fluid Mech.* **54**, 263–288.
- RIBEIRO, M. M. 1972 Turbulent mixing of coaxial jets. Mast. of Science thesis, Imperial College of Science and Technology, London.
- RICOU, F. P. & SPALDING, D. B. 1961 Measurement of entrainment by axisymmetrical turbulent jets. *J. Fluid Mech.* **11**, 21–32.
- RODI, W. 1972 The prediction of free turbulent boundary layers by use a two equation model of turbulence. Ph. D. thesis, University of London.
- SAMIMY, M., REEDER, M. F. & ELLIOT, G. S. 1992 Compressibility effects on large structures in free shear flows. *Phys. Fluids A* **4**, 1251–1258.
- SARKAR, S., ERLEBACHER, G., HUSSAINI, M. Y. & KREISS, H. O. 1991 The analysis and modelling of dilatational terms in compressible turbulence. *J. Fluid Mech.* **227**, 473–493.
- SCHADOW, K. C., GUTMARK, E. & WILSON, K. J. 1989 Passive mixing control in supersonic coaxial jets at different convective Mach numbers. *AIAA Paper*, 89-0995.
- SCHAFFAR, M. & BOBIN, L. 1976 Recherche de structures cohérentes dans un jet froid au moyen de corrélations. *Rapport 130/76*, Institut Franco-Allemand, Saint-Louis.
- SOKOLOV, M., KLEIS, S. J. & HUSSAIN, A. K. M. F. 1981 Coherent structures induced by two simultaneous sparks in an axisymmetric jet. *AIAA J.* **19**, 1000–1008.
- STROMBERG, J. L., MCLAUGHLIN, C. K. & TROUTT, T. R. 1980 Flow field and acoustic properties of a Mach number 0.9 jet at a low Reynolds number. *J. Sound Vibration* **72**, 159–176.
- TAM, C. K. W. & HU, F. Q. 1989 On the three families of instability waves of high speed jets. *J. Fluid Mech.* **201**, 447–483.
- THOMPSON, K. W. 1987 Time dependent boundary conditions for hyperbolic systems. *J. Computational Physics* **68**, 1–24.
- VERZICCO, R. & ORLANDI, P. 1994 Direct simulations of the transitional regime of a circular jet. *Phys. Fluids A* **6**, 751–759.
- WINANT, C. D. & BROWAND, F. K. 1974 Vortex pairing : the mechanism of turbulent mixing layer growth at moderate Reynolds number. *J. Fluid Mech.* **63**, 237–255.
- ZHOU, Z. W. & LIN, S. P. 1992 Absolute and convective instability of a compressible jet. *Phys. Fluids A* **4**, 277–282.